

2018-11

Fine-scale hydrodynamic metrics underlying predator occupancy patterns in tidal stream environments

Lieber, L

<http://hdl.handle.net/10026.1/11842>

10.1016/j.ecolind.2018.06.071

Ecological Indicators

Elsevier BV

All content in PEARL is protected by copyright law. Author manuscripts are made available in accordance with publisher policies. Please cite only the published version using the details provided on the item record or document. In the absence of an open licence (e.g. Creative Commons), permissions for further reuse of content should be sought from the publisher or author.

1 **Fine-scale hydrodynamic metrics underlying predator occupancy patterns in**
2 **tidal stream environments**

3

4 Lilian Lieber^{1*}, W. Alex M. Nimmo-Smith², James J. Waggitt³, Louise Kregting¹

5

6 ¹School of Natural and Built Environment, Queen's University Marine Laboratory, 12-13 The Strand,

7 Portaferry, BT22 1PF, Northern Ireland, UK

8 ²Marine Institute, University of Plymouth, Drake Circus, Plymouth, PL4 8AA, England, UK

9 ³School of Ocean Sciences, Bangor University, Menai Bridge, Anglesey, LL59 5AB, UK

10

11 *Corresponding author:

12 Lilian Lieber

13 Queen's University Marine Laboratory

14 12-13 The Strand

15 Portaferry BT22 1PF

16 Northern Ireland, UK

17 Email: l.lieber@qub.ac.uk

18 Tel: 0044 (0) 28 4272 7806

19

20

21

22

23

24

25

26 **Abstract**

27 Whilst the development of the tidal stream industry will help meet marine renewable energy (MRE)
28 targets, the potential impacts on mobile marine predators using these highly dynamic environments
29 need consideration. Environmental impact assessments (EIAs) required for potential MRE sites
30 generally involve site-specific animal density estimates obtained from lengthy and costly surveys.
31 Recent studies indicate that whilst large-scale tidal forcing is predictable, local hydrodynamics are
32 variable and often result in spatio-temporal patchiness of marine predators. Therefore,
33 understanding how fine-scale hydrodynamics influence animal distribution patterns could inform the
34 placing of devices to reduce collision and displacement risks. Quantifying distributions requires
35 animal at-sea locations and the concurrent collection of high-resolution hydrodynamic
36 measurements. As the latter are routinely collected during tidal resource characterization at
37 potential MRE sites, there is an untapped opportunity to efficiently collect information on the
38 former to improve EIAs. Here we describe a survey approach that uses vessel-mounted ADCP
39 (Acoustic Doppler current profiler) transects in combination with marine mammal surveys to collect
40 high-resolution and concurrent hydrodynamic data in relation to pinniped (harbour seals *Phoca*
41 *vitulina*, grey seals *Halichoerus grypus*) at-sea occupancy patterns within an energetic tidal channel
42 (peak current magnitudes $>4.5\text{ms}^{-1}$). We identified novel ADCP-derived fine-scale hydrodynamic
43 metrics that could have ecological relevance for seals using these habitats. We show that our local
44 acoustic backscattering strength metric (an indicator for macro-turbulence) had the highest
45 influence on seal encounters. During peak flows, pinnipeds avoided the mid-channel characterized
46 by extreme backscatter. At-sea occupancy further corresponded with the increased shear and eddies
47 that are strong relative to the mean flows found at the edges of the channel. Our approach,
48 providing oceanographic context to animal habitat use through combined survey methodologies,
49 enhances environmental management of potential MRE sites. The cost-effective collection of such
50 data and the application of our metrics could streamline the EIA process in the early stages of the
51 consenting process.

52

53 **Keywords:** Acoustic Doppler current profiler, acoustic backscatter, physical drivers, environmental
54 impact assessment, marine renewable energy, pinniped

55 **1. Introduction**

56 The global drive towards marine renewable energy (MRE) extraction has led to a rapid
57 increase in planned tidal turbine installations in coastal areas experiencing high ($>2\text{ms}^{-1}$) current
58 speeds (Fraenkel 2004). Whilst the exploitation of tidal stream energy will help reach renewable
59 energy targets, the potential impacts on animals using these habitats must be considered in
60 recognition of marine licensing and legislation. A variety of mobile marine predators (cetaceans,
61 pinnipeds, seabirds) exploit tidally energetic environments for foraging opportunities (Benjamins et
62 al., 2015a). However, there is still a large degree of uncertainty surrounding interactions between
63 predators and tidal devices. A range of potential impacts have been identified including collisions
64 with moving components, displacement from foraging areas and changes in foraging efficiency and
65 locomotive costs due to possible alteration of flow fields around array installations (Shields et al.
66 2011; Fox et al., 2017). To protect against these risks, environmental impact assessments (EIA) are
67 generally required in the consenting process, where potential risks are identified, and mitigation
68 measures established before developments commence. In many parts of the world, developers are
69 tasked by regulators to undertake marine mammal site characterizations (e.g. boat-, plane- or shore-
70 based surveys) as part of EIAs (Wilson et al., 2007; Savidge et al., 2014). These surveys are aimed at
71 generating baseline data of marine mammal presence to eventually derive site-specific absolute
72 abundance or density estimates (Benjamins et al., 2015b). However, despite the high cost and time
73 involved in these surveys, the density estimates generally have high levels of uncertainty due to the
74 complexity of ecological systems (Harwood and Stokes, 2003).

75 A different approach is to understand how animals use these energetic tidal environments
76 in relation to hydrodynamic forcing and fine-scale variations in vertical profiles. Flow regimes are not
77 homogenous in tidal environments and vary owing to the occurrence of fine-scale, tidally-driven or
78 bathymetry-induced physical processes, including shear boundaries, eddies and boils (Nimmo-Smith
79 et al., 1999; Evans et al., 2013; Jones et al., 2014; Kregting et al., 2016). This heterogeneity creates
80 spatial and temporal variation in the distribution of species, with marine predators regularly

81 associated with certain tidal velocities and physical processes (Johnston et al., 2005; Embling et al.,
82 2012; Jones et al., 2014; Waggitt et al., 2016a; Waggitt et al., 2016b; Benjamins et al., 2016;
83 Benjamins *et al.*, 2017). Therefore, quantifying spatio-temporal variation in animal site usage in
84 relation to hydrodynamic features may help to identify which and when areas may be used (Zamon
85 2001; Waggitt & Scott 2014; Benjamins et al., 2015b; Hastie et al., 2016; Waggitt et al., 2017a). This
86 can provide developers with valuable information prior to array installation to reduce the risk of
87 collision and displacement. This information can also predict changes in distributions caused by
88 potential alterations in the hydrodynamic regime around installations (Shields et al. 2011).

89 Tidal resource characterization generally marks the early stages of an MRE project to
90 quantify the physical properties of the site, estimate potential energy generation and evaluate the
91 placing of devices (Polagye & Thomson 2013). Acoustic Doppler current profilers (ADCPs) are
92 instruments designed to measure current velocities (speed and direction) and flow structures
93 throughout the water column and are widely used during MRE resource characterization to capture
94 the local flow dynamics over a range of spatial and temporal scales (Evans et al., 2013). ADCPs can
95 either be bottom-mounted to measure a flow's temporal variation at a specific location (Lu & Lueck
96 1999), or vessel-mounted to infer spatial variation in velocities across a site (Simpson et al., 1990).
97 To capture fine-scale spatial heterogeneity, it has been demonstrated that vessel-mounted ADCP
98 surveys can provide valuable means to characterize tidal energy sites, overcoming the need to
99 deploy high-resolution grids of moored ADCPs across a site (Fong & Monismith 2004; Epler et al.,
100 2010; Evans et al., 2013; Goddijn-Murphy et al., 2013; Savidge et al., 2014).

101 With extensive resources allocated towards MRE resource characterization, there currently
102 appears to be an untapped resource for combined survey methodologies that could be adapted for
103 EIAs to assess risks to marine mammals. Specifically, vessel-mounted ADCP surveys could provide a
104 platform to collect fine-scale data on marine mammal at-sea distribution patterns in relation to
105 concurrently measured tidally-induced physical features.

106 In this study, we aimed to combine surveys of at-sea occupancy patterns of two pinniped
107 species known to exhibit tidal patterns in their distributions (harbour seals *Phoca vitulina* and grey
108 seals *Halichoerus grypus*) in relation to concurrently collected, high-resolution hydrodynamic data.
109 The study was performed in a highly dynamic, restricted tidal channel located in Strangford Lough,
110 Northern Ireland. Characterized by depth-averaged current magnitudes exceeding 4ms^{-1} during
111 spring tides, the channel is frequently exploited as a tidal turbine test site (Jeffcoate et al., 2016).

112 Using vessel-mounted ADCP transects, data were collected during a spring and neap tidal
113 cycle to fulfil two main objectives. Firstly, we sought to measure high-resolution spatial and
114 temporal variations in hydrodynamic conditions to visualize and quantify novel fine-scale metrics of
115 physical processes to provide oceanographic context to animal site usage (macro-turbulence, eddies
116 and shear). Secondly, to test the ecological relevance of these metrics by comparing their
117 explanatory power to inform at-sea pinniped distributions to that of more commonly-used
118 measurements in tidal stream environments (current magnitude, depth and time to high water).

119 **2. Material and Methods**

120 *2.1 Study site*

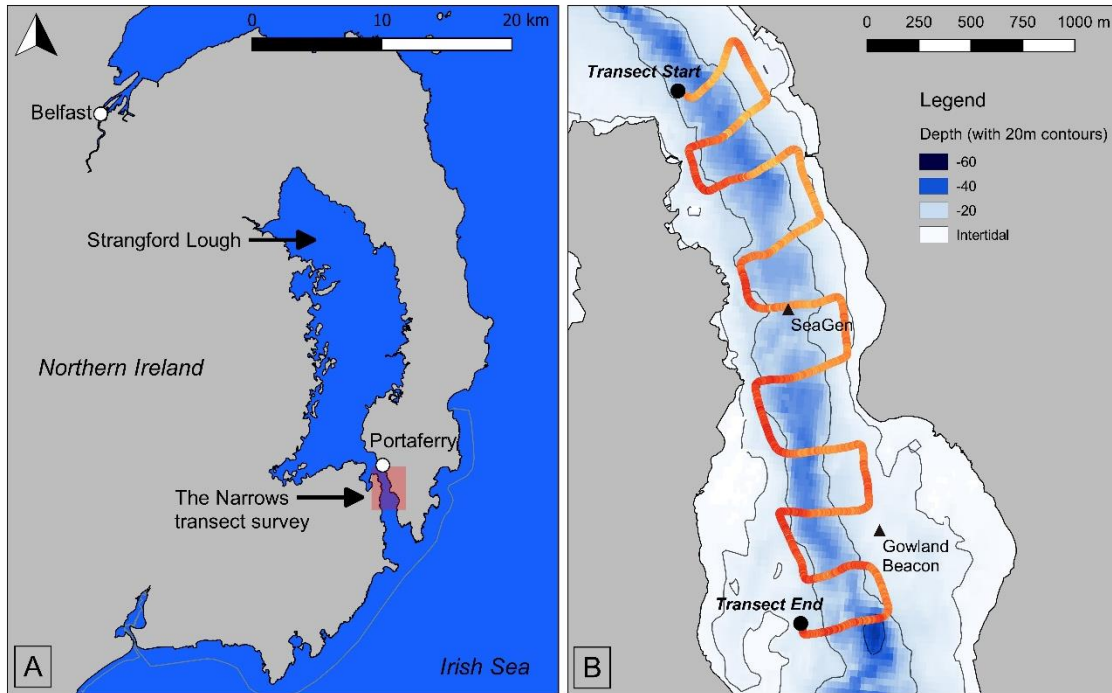
121 The survey was performed within the Narrows, a tidal channel linking Strangford Lough to
122 the Irish Sea, located on the east coast of Northern Ireland, UK (Fig. 1). The Narrows are
123 approximately 8km long with a minimum width of 1km and depth varying between 30-60m in the
124 mid-channel, with kelp beds present along the edges of the channel down to approximately the 15m
125 depth contour.

126

127

128

129

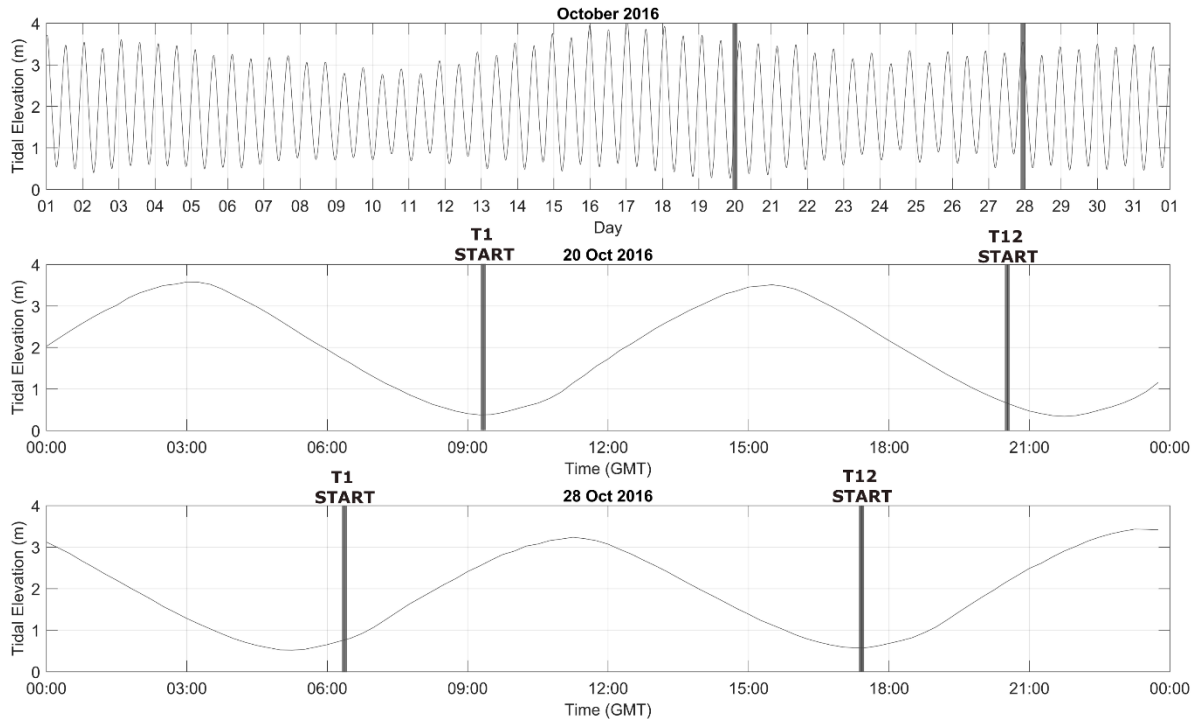


130 **Figure 1:** (A) Map showing the study area within the Narrows, a tidal channel located in Strangford Lough, Northern
 131 Ireland, UK, highlighted by a red box. (B) Path of a representative vessel-mounted ADCP transect (Transect 1, 20 October
 132 2016) performed within the Narrows colored by ADCP-derived sea surface temperature (°C). Note, small cross-channel
 133 variation in temperatures (min=13.18°C, yellow; max=13.98°C, red) are visible due to different rates of advection and
 134 vertical mixing.

135 Data were collected over two semi-diurnal tidal cycles (approximately 12 hours per cycle)
 136 during a spring (progression from springs to neaps) and a neap (progression from neaps to springs)
 137 tide on October 20th and 28th 2016, respectively (Fig.2). Strangford Lough is a designated Special
 138 Area of Conservation, with the harbour seal, listed on Annex II of the EC Habitats Directive,
 139 presenting a qualifying feature. The study was conducted following the species' breeding and
 140 moulting season (timings vary but *P. vitulina* pupping is generally in June/July, with moulting
 141 thereafter in July/August). During the time of the survey, the UK's first full-scale tidal turbine,
 142 SeaGen, installed in the Narrows in 2008, was non-operational and there were no other turbines
 143 under test within the area covered by transects.

144

145



146 **Figure 2:** Tidal regime shown for the month of October 2016 from a tide gauge located at Portaferry Pier (top panel) with
 147 lines highlighting the spring and neap tidal survey days on 20 and 28 October 2016, respectively. The middle and bottom
 148 panel show the semi-diurnal tidal cycle during each survey, with grey lines marking the start of Transect 1 and 12 (T1; T12)
 149 for each survey day.

150 *2.2 Transect design*

151 Repeat parallel-line transects were performed onboard a 10.5m long offshore-coded vessel
 152 (The Cuan Shore, Cuan Marine Services Ltd) travelling at a constant vessel speed of 5 knots, during a
 153 sea state of 0-1 and a visibility of 6-10km (Fig. 1). This setup allowed for controlled vessel movement
 154 and comparable data acquisition conditions across surveys. Transects were run perpendicular to the
 155 dominant flow direction and made up of square, parallel transect lines rather than zig zag lines to 1)
 156 maximize coverage across the varying current fields, 2) better identify small-scale hydrodynamic
 157 features along the edges of the channel, and 3) avoid an overestimation in velocity in the direction
 158 of the boat (Fong & Monismith 2004). A total of 24 transects (240 lines) were performed where each
 159 transect started from the same point and consisted of 10 lines (each line= \sim 450 m) at \sim 300 m
 160 spacing, covering an approximate area of 2900 m x 450 m (along-track distance= \sim 7000 m). Transects

161 were repeated 12 times at hourly intervals over a tidal period starting at low water on 20 October
162 2016 and one hour after low water on 28 October 2016 (Fig. 2).

163 *2.3 CTD and tidal elevation*

164 To assess stratification and the speed of sound in the Narrows, twelve conductivity-
165 temperature-depth (CTD) profiles were collected throughout the neap survey day, 28 October 2016,
166 using a Valeport CTD (model 602) at the start and end of every second transect in the mid-channel
167 (Table S1, Supplementary Information). Tidal elevation data was extracted from a monitoring (>3
168 months) tide gauge located at the Portaferry Pier in the Narrows, Strangford Lough.

169 *2.4 Acoustic Doppler Current Profiler (ADCP) collection and post-processing*

170 A pole-mounted RDI Workhorse Monitor broadband ADCP in bottom-tracking mode was
171 used for the transect surveys. The ADCP was mounted on the starboard side of the vessel at 1.15m
172 depth with its sensors checked and internal compass calibrated on the boat prior to the survey. The
173 ADCP's operating frequency was 600kHz and it was configured to ping at 1Hz with an ensemble
174 interval of 1 second and a vertical bin size (cell depth size of averaged data) of 1m (ambiguity
175 velocity=3.8 m/s). An on-board differential GPS system (Hemisphere) was linked to the incoming
176 ADCP data stream acquired with VMDas software (v. 1.46; RD Instruments, Inc.) to provide
177 navigational information during transects.

178 As part of the standard quality control procedures, ADCP data was post-processed in
179 WinADCP (v. 1.14; RD Instruments, Inc.) using default parameters for vertical, horizontal and error
180 velocities, percent good pings, beam correlation, and surface or bottom reflection; and data was
181 checked for anomalous pitch and roll. True water velocities were computed by subtraction of the
182 bottom-tracked boat velocity. Depth-averaged velocity vectors were plotted over transect lines to
183 visualize areas of variable flow such as eddies and flow reversals. These were then quantified as
184 'Relative Variance in Velocity' (*RelVarVel*), a bin-averaged (horizontally and vertically) velocity
185 covariate later used in modelling. For this, within 1min-binned time intervals along a given transect,

186 the sum of the standard deviation of the depth-averaged northward and eastward velocity
187 components was divided by mean current magnitude, resulting in a parameter describing the
188 horizontal variance in current velocity relative to the strength of the flow at the given location. This
189 parameter increases in variable weak flows (relatively strong eddies in areas of low currents).

190 Further, vertical shear (S) was calculated across 1m vertical intervals along each transect
191 using the following equation:

$$192 \quad S = ((du/dz)^2 + (dv/dz)^2)^{1/2}$$

193 where du/dz and dv/dz are the vertical gradients in the east and the north velocity components,
194 respectively.

195 High values of scattering, or echo intensity, can be associated with zooplankton, fish,
196 suspended sediment or turbulence, such as enhanced surface bubble entrainment indicative of
197 macro-turbulence (Brierley et al., 1998; Nimmo-Smith et al., 1999; Demer et al., 2000; Lavery et al.,
198 2009). In tidal channels, it is likely that the scattering source is dominated by the latter. Therefore, to
199 quantify the acoustic scattering in the water column as a metric for macro-turbulence, volume-
200 backscattering strength (S_v , measured in decibels, dB) was calculated over a finite volume
201 (maximum of 40 bins) from the ADCP's recorded raw echo intensity data using a working version of
202 the sonar equation as described in Deines (1999). S_v has been evaluated separately for each bin
203 along each of the four beams of the ADCP. For each range bin, the maximum of the four beams
204 ($S_{v_{max}}$) was taken to create depth profiles of the maximum level of scattering through the water
205 column.

206 *2.5 Marine mammal transect survey design*

207 Constant effort (continuous search effort) surveys for marine mammals were conducted
208 throughout eight of the 12 transects (omitting hours of darkness) during both survey days with
209 resting times in between transects (when steaming back to the starting point) to avoid observer
210 fatigue. Observations were made from the front deck of the vessel (3m above water level), capturing

211 a 300 m-wide transect on either side ($\pm 90^\circ$) and ahead of the vessel. Sightings were made by the
212 naked eye and identified to species level using binoculars when required. Time and position of
213 sightings were recorded using a handheld GPS (Garmin GPSMAP 78). The relative bearing in degrees
214 ($^\circ$) from the vessel was noted using mounted angle boards, and radial distance to the animal was
215 estimated by eye with the help of available landmarks and the use of rangefinder binoculars.
216 Environmental data (sea state and visibility) were recorded at the start of each new transect or when
217 conditions changed. A total transect distance of 117.23 km was covered during the marine mammal
218 surveys, with an average transect length of 7.33 km (SD=322.58 m). Overall observer effort
219 comprised 11.4 hours with an average transect duration of 43 min (SD=5.26 min). The sighting data
220 reported in this study present a measure of relative sea usage rather than absolute numbers or
221 densities. Further, the number of independent observations was insufficient to apply the detection
222 function to obtain robust animal density estimates (Buckland et al. 2001; Thomas et al. 2010).

223 *2.6 Marine mammal data analysis*

224 Generalized additive models (GAMs: Wood 2006) with a binomial error distribution and a
225 'logit' link function were used to quantify the relationship between the probability of encountering a
226 seal (grey or harbour) and hydrodynamic measurements. GAMs construct a series of polynomial
227 curves showing quantifying relationships between the response and explanatory variables, with each
228 polynomial curve focusing upon a different range of the explanatory variable. over different ranges
229 of the latter. These polynomial curves are joined together at a series of locations known as knots,
230 enabling non-linear relationships between explanatory and response variables to be quantified. As
231 non-linear relationships were expected, GAMs were preferred over Generalized Linear Models
232 (GLM) (Wood, 2006).

233 Combinations of current direction, speed and depth indirectly detect the presence of
234 hydrodynamic features. For instance, turbulent-structures often occur in shallow and fast-water in
235 the wake of islands/headlands (Benjamins et al., 2015). However, the ADCP-derived measurements

236 should directly detect these hydrodynamic features. Statistical analyses investigated whether direct-
237 measurements of turbulent structures were better at explaining variance in the presence of seals
238 than indirect-measurements of these hydrodynamic features. Two different sets of models were
239 performed. The first set of models consisted of three explanatory variables commonly used to
240 explain animal distributions in tidal stream environments (e.g. Hastie et al., 2016; Waggitt et al.,
241 2016a): time to high tide (*M2HT*), depth-averaged current magnitude (*Mag*) and depth. These
242 explanatory variables were combined in a single model. Backwards model selection was performed
243 thereafter, with only significant ($p < 0.05$) explanatory variables retained in the final model (Zuur
244 2010). The second set of models used novel explanatory variables derived from concurrent ADCP
245 measurements: backscattering strength (*Sv_{max}*), mean relative variance in velocity (*RelVarVel*) and
246 maximum shear (*MaxS*). As these explanatory variables quantify similar hydrodynamic features,
247 shown by strong collinearity (Fig. S1, Supplementary Information), these were modelled separately.
248 This approach allowed the performance of each novel explanatory variable to be directly compared
249 to the set of more conventional explanatory variables. The number of knots was constrained to 3 to
250 avoid overfitting and test for ecologically interpretable relationships (Waggitt et al. 2016b). The
251 exception was *M2HT* where the number of knots was constrained to 6, as more complicated
252 relationships were expected across the ebb-flood cycle. Distance (m) travelled per minute was also
253 included as an offset to account for differences in the area covered among samples. Further
254 information on response and explanatory variables is provided below. GAMs were performed in R
255 (v.3.1.1; R Core Team 2013) using the 'mgcv' package (v. 1.8-12; Woods 2017).

256 The response variable was the presence or absence of seals per minute. Rather than simply
257 matching the timing of the sighting (*Presence*) to the ADCP 1-minute bin-averaged period, the
258 positional data point of the sighting (corrected for distance and bearing) was taken and matched to
259 the nearest bottom-tracked latitude/longitude waypoint along the transect (spatial rather than
260 temporal matching). This was done by calculating the distance from the sighting to all waypoints
261 along the track and finding the nearest distance. This approach is more robust than temporal

262 matching by extracting the physically nearest environmental parameters experienced by the seal.
263 This provided the highest resolution match in space because seals were often seen prior to the
264 vessel's closest point of approach to the seal's position.

265 The explanatory variables were the mean or maximum values of hydrodynamic water
266 column measurements per minute. The mean was calculated for water depth (in meters), time to
267 high tide (in minutes), depth-averaged current magnitude (in meters per second) and relative
268 variance in velocity (*RelVarVel*, in meters per second); the maximum values of vertical shear and
269 volume backscattering strength (S_v in dB re 1m^{-1}) were calculated per minute. The use of maximum
270 rather than mean values meant that fine-scale, but prominent hydrodynamic features associated
271 with high vertical shear and backscattering strength would be identified. All explanatory variables
272 were modelled as non-linear terms.

273 Residuals showed no evidence of spatial or temporal autocorrelation, so additional
274 statistical approaches to account for this (e.g. mixed effect models, general estimating equations)
275 were deemed unnecessary. Relationships between the probability of encountering seals and each
276 explanatory variable were then estimated from model parameters. In these estimations, the
277 explanatory variable of interest was varied between its minimum and maximum value, whilst others
278 were held at their mean value. An effect size was obtained by dividing the absolute difference
279 between the minimum and maximum predicted values by the minimum predicted value. The
280 calculation of a standardized effect size allowed the relative influence of different explanatory
281 variables to be directly compared (Waggitt et al., 2017b). This standardized effect size was then used
282 to compare the relative influence of explanatory variables.

283 **3. Results**

284 *3.1 Hydrodynamics*

285 Contour plots of an entire transect during minimum flow velocities (slack low water, transect
286 1; Fig. 3a) and as a comparison, at times of maximum flow velocities (peak flood, transect 4; Fig. 3b),
287 are given for two representative time-series during the spring tide survey. Throughout the ADCP

288 transects, higher current speeds were recorded during the flooding tide compared to the ebbing
289 tide, as well as during the spring survey compared to the neap survey. This is in accordance with the
290 asymmetry of the tidal cycle (shorter flood, and longer ebb periods, respectively) and hydrodynamic
291 model predictions (Kregting & Elsäßer 2014). Generally, strongest flow velocities were recorded in
292 the central parts of the channel compared to the edges, with pronounced fine-scale variability in
293 tidal velocity, shear and acoustic backscatter (a metric for macro-turbulence) as a response to the
294 channel's bathymetry (Fig. 3b). Patches of high vertical shear were found near the bed in the central
295 part of the channel associated with the strongest flows there, but also in regions of rapidly changing
296 bathymetry towards the sides of the main channel, over the 20m depth contour.

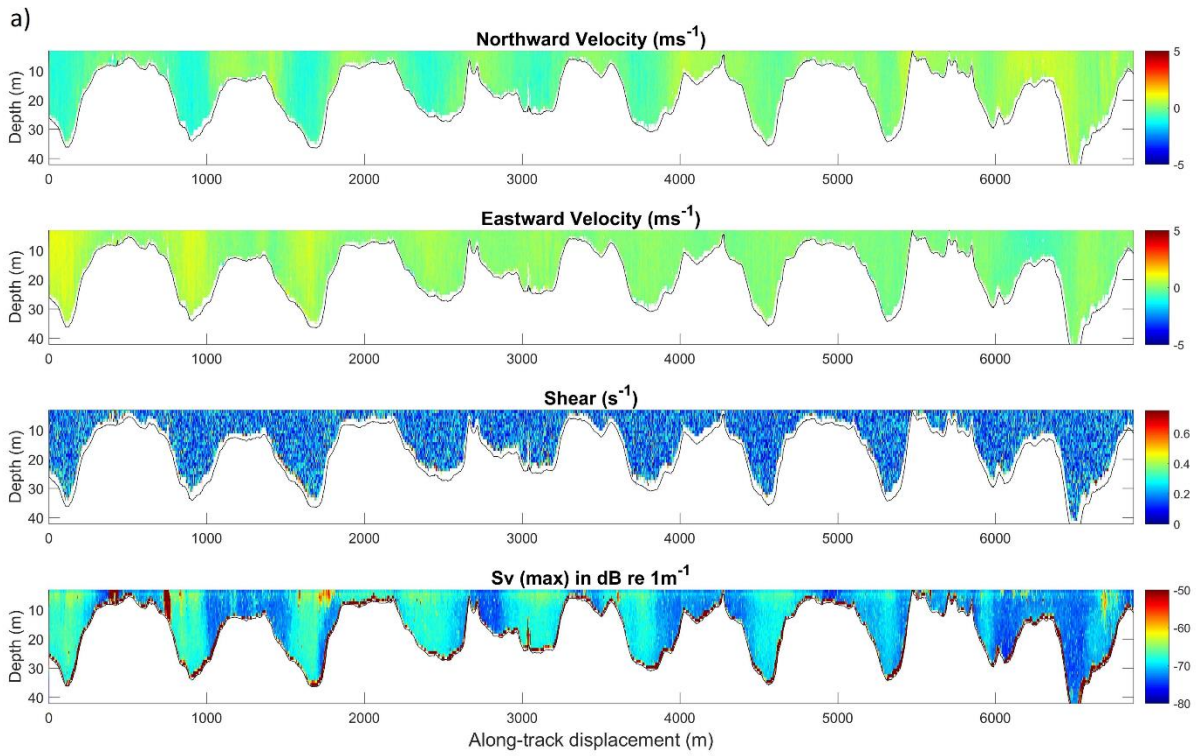
297

298

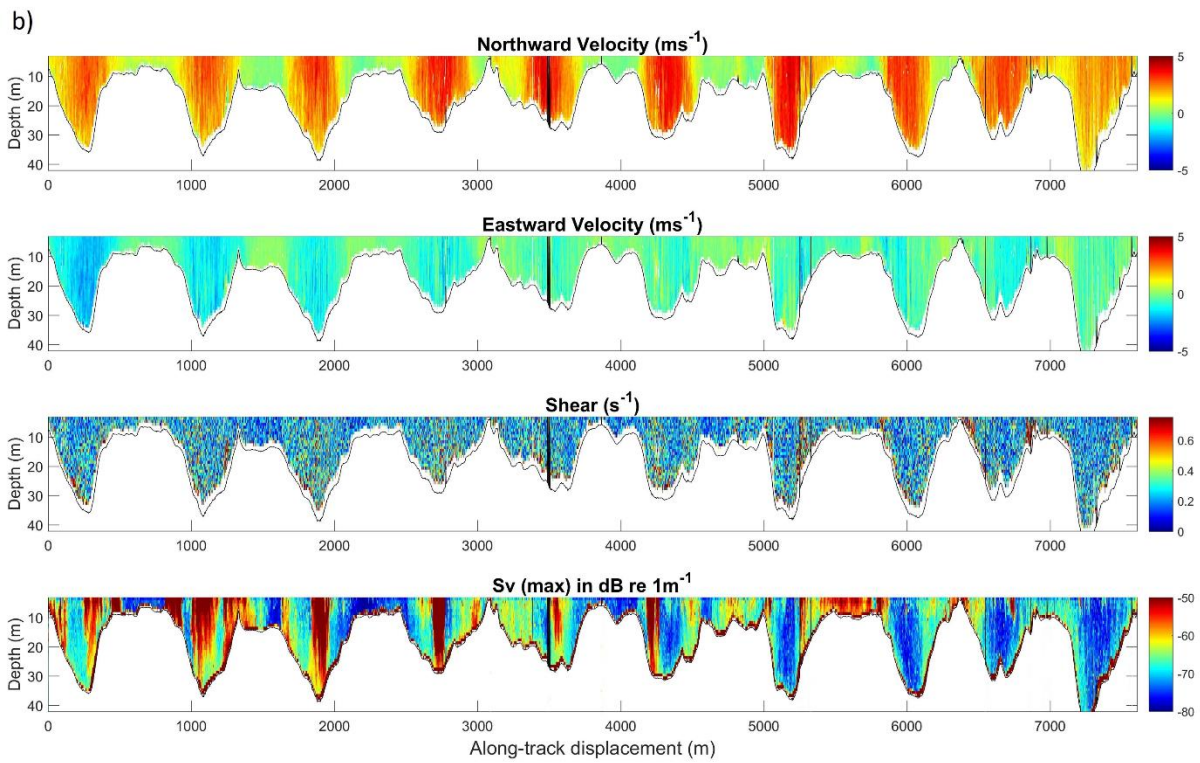
299

300

301



302

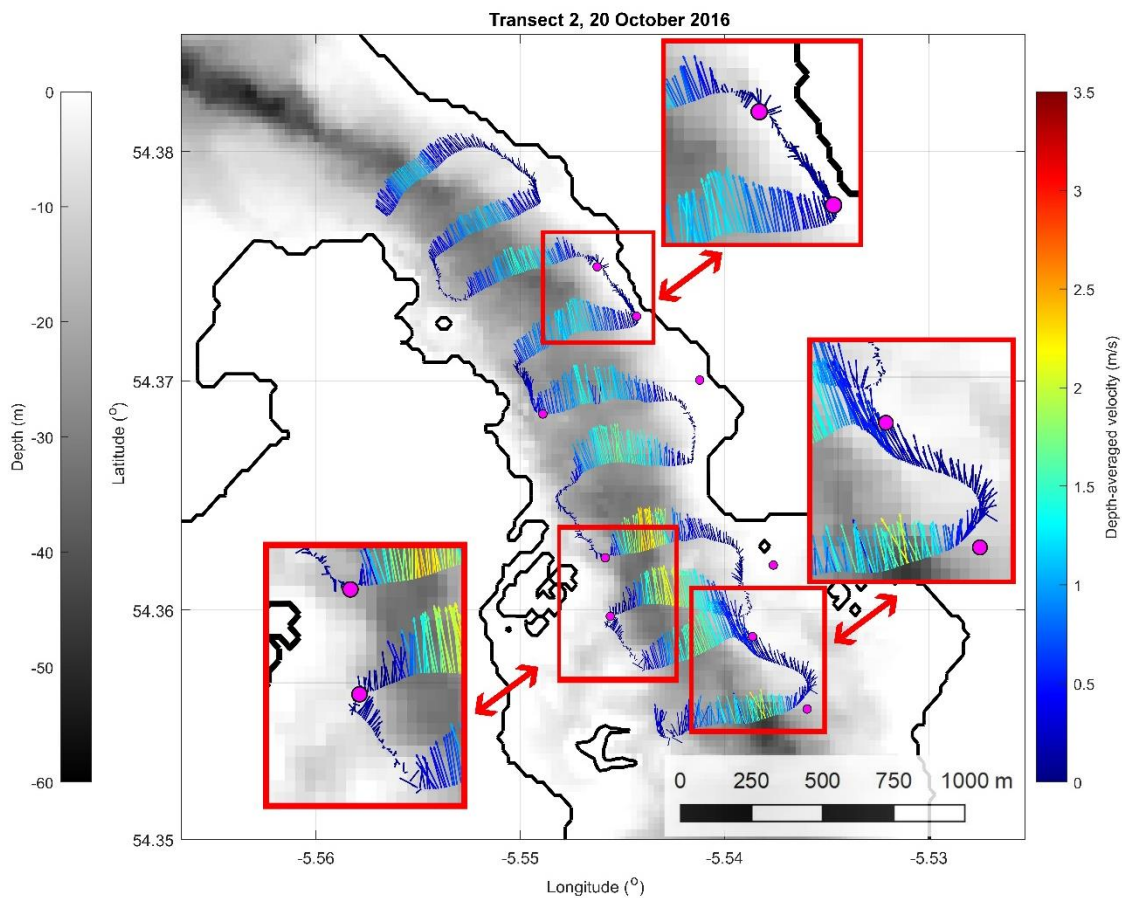


303 **Figure 3:** Vertical sections recorded by the ADCP along an entire transect during low water slack (a; Transect 1, spring tidal

304 survey on 20 October 2016, 41min duration) and peak flood tide (b; Transect 4, spring tidal survey on 20 October 2016,

305 48min duration), respectively. Note, the black vertical line at 3500m along-track distance indicates short-term data loss.

306 The distribution of backscatter (Sv_{max}) was even more variable between low and high flow
 307 condition. For instance, during periods of weak flow, higher values of Sv_{max} were typically associated
 308 with the central channel indicating residual turbulence may have held material in the water column,
 309 such as micro-bubbles entrained from the surface and sediment re-suspended from the bed. During
 310 peak flow, regions of extremely high Sv_{max} were found extending from the surface down towards the
 311 seabed in the central part of the channel, supporting our assertion that Sv is an indicator of macro-
 312 turbulence (entrained air) rather than plankton or fish.



313 **Figure 4:** Typical plot of depth-averaged velocity vectors (current direction indicated by vectors and velocity magnitude by
 314 color; see color bar) during flooding tide (Transect 2; spring tidal survey on 20 October 2016). Fastest flows are observed in
 315 the mid-channel with fine-scale hydrodynamic features, such as eddies, visible around the edges of the channel (red
 316 inserts). Filled dots mark seal sightings corrected for range and bearing.

317 There was a clear rectilinear flow pattern in the channel with flow vectors aligned with the
 318 mean longitudinal direction of the central part of the channel. However, there was more variability
 319 in the direction of the weaker flows in the shallow areas of the channel. This became apparent when

320 visualizing velocity vectors showing local flow reversals towards the edges of the channel (Fig. 4).
321 These reversals correspond to the presence of eddies and other turbulent features being more
322 pronounced, relative to the magnitude of the local mean flow, in these shallow areas. Finally, there
323 was no evidence for vertical stratification due to temperature ($T^{\circ}\text{C} = 13.53$ (SD=0.14) or salinity
324 (34.15 PSU (SD=0.13) in the mid-channel as identified by the CTD stations.

325 *3.2 Seal at-sea distribution*

326 **3.2.1 Observational Surveys**

327 The total number of seal sightings was 34 (23 grey and 11 harbour seals) during the spring
328 and 18 (14 grey and 4 harbour seals) during the neap tidal survey, respectively, totaling 52 sightings.
329 Overall, the mean number of seals sighted during each transect was 3.3 (SD=2.1), ranging from 0-9
330 observations. The spatio-temporal distribution and numbers of seal sightings is shown in Figure 5
331 and Table 1, while the spatial distribution of selected, ADCP-derived variables is plotted in Figure 6.

332

333

334

335

336

337

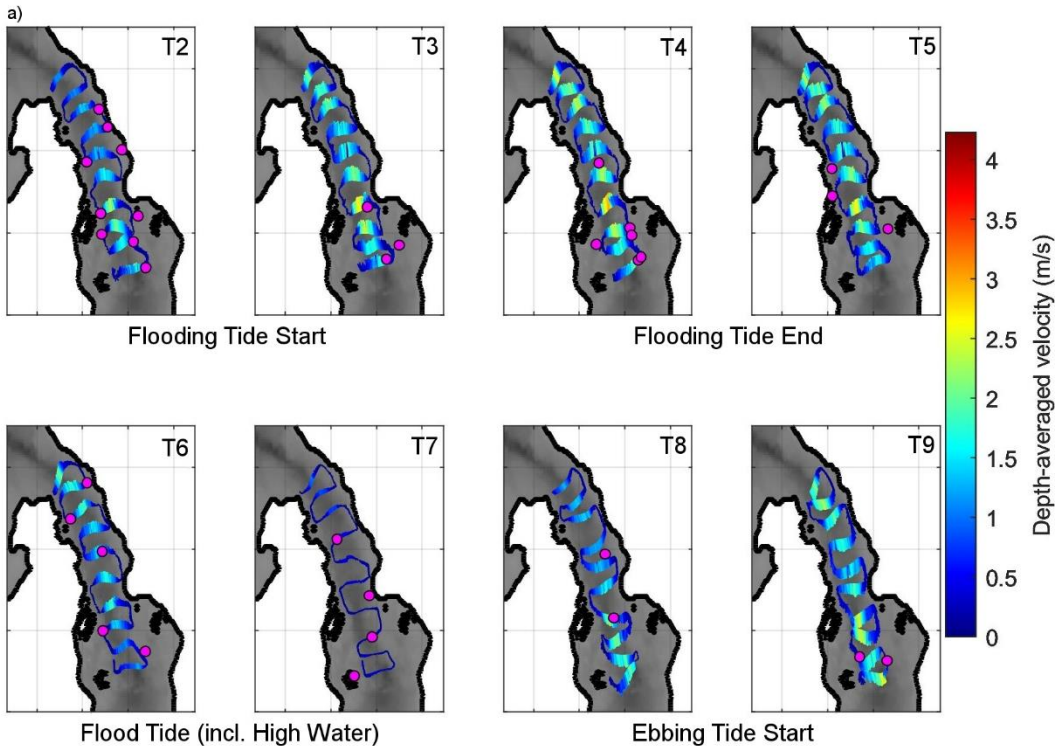
338

339

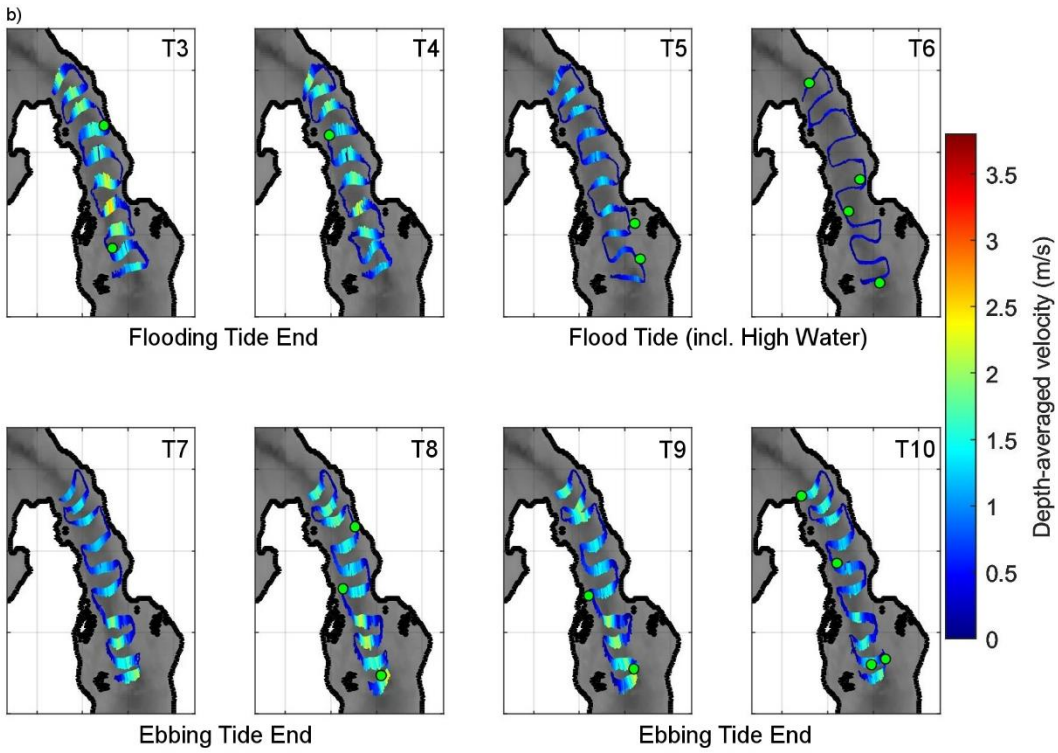
340 **Table 1:** Detailed transect information during both the spring (20 October 2016) and neap (28 October 2016) tidal survey,
 341 in the Strangford Narrows. Sea State (=0-1) and Visibility (6-10km) were constant for all transects. Transects used
 342 for pinniped observations are highlighted in bold. Approximate tidal state is indicated with hours after low water
 343 (LW) and high water (HW).

Date	Transect number	Transect start time (GMT)	Transect end time (GMT)	Transect Duration (min)	Observer Effort	# Seal Encounters	Tidal State (approx.)
20-10-16	1	9:20	10:01	0:41	OFF	NA	LW
20-10-16	2	10:20	11:09	0:49	ON	9	LW +1
20-10-16	3	11:20	12:08	0:48	ON	3	LW +2
20-10-16	4	12:20	13:07	0:47	ON	6	LW +3
20-10-16	5	13:22	14:04	0:42	ON	3	LW +4
20-10-16	6	14:20	15:06	0:46	ON	5	LW +5
20-10-16	7	15:22	16:02	0:40	ON	4	HW
20-10-16	8	16:21	17:03	0:42	ON	2	HW +1
20-10-16	9	17:19	18:13	0:54	ON	2	HW +2
20-10-16	10	18:35	19:21	0:46	OFF	NA	HW +3
20-10-16	11	19:35	20:17	0:42	OFF	NA	HW +4
20-10-16	12	20:32	21:13	0:41	OFF	NA	HW +5
28-10-16	1	6:22	7:10	0:48	OFF	NA	LW +1
28-10-16	2	7:21	8:04	0:43	OFF	NA	LW +2
28-10-16	3	8:23	9:02	0:39	ON	2	LW +3
28-10-16	4	9:20	10:02	0:42	ON	1	LW +4
28-10-16	5	10:20	11:02	0:42	ON	2	LW +5
28-10-16	6	11:20	11:59	0:39	ON	4	HW
28-10-16	7	12:20	13:00	0:40	ON	0	HW +1
28-10-16	8	13:31	14:16	0:45	ON	3	HW +2
28-10-16	9	14:38	15:17	0:39	ON	2	HW +3
28-10-16	10	15:40	16:14	0:34	ON	4	HW +4
28-10-16	11	16:35	17:08	0:33	OFF	NA	HW +5
28-10-16	12	17:25	18:10	0:45	OFF	NA	LW

344

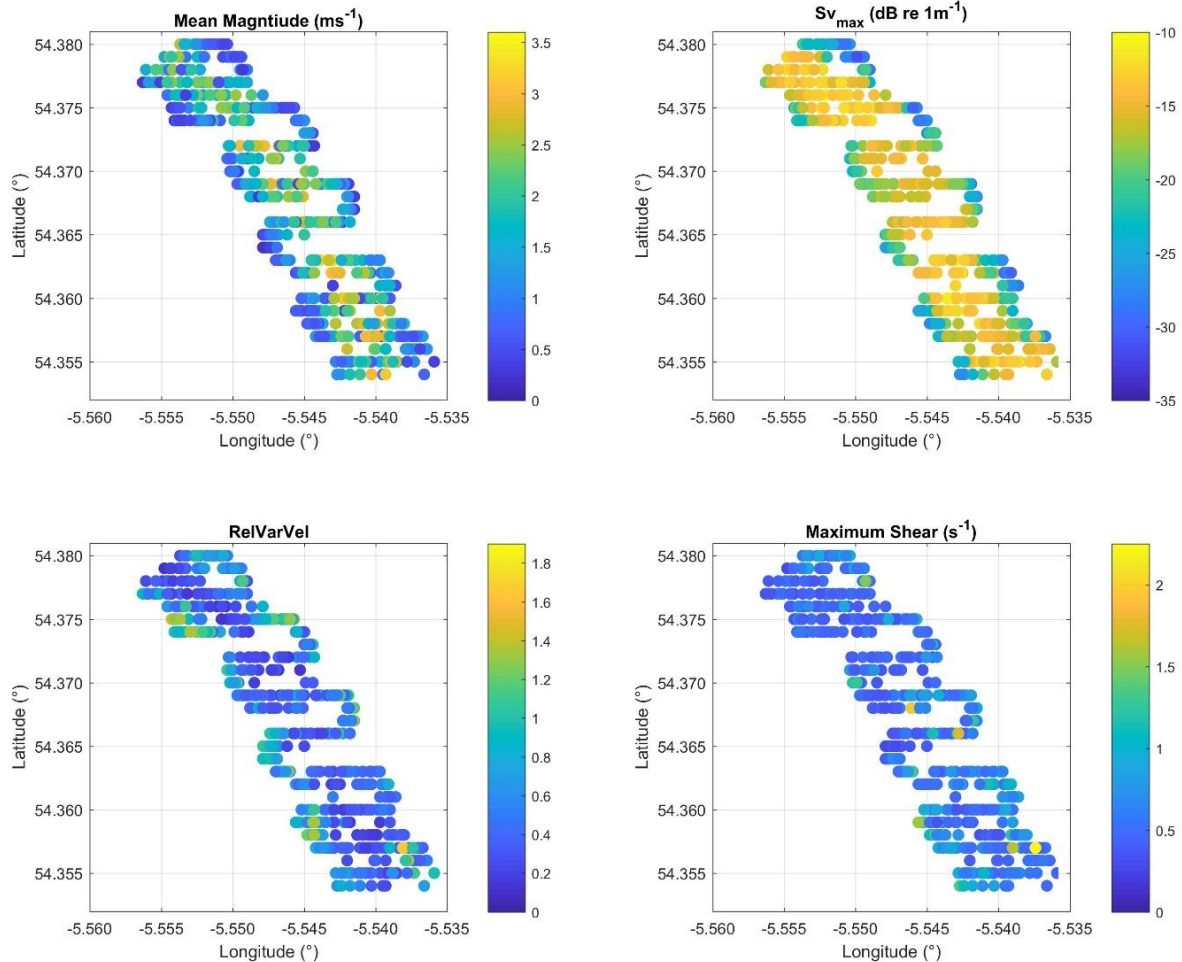


345



346

347 **Figure 5:** Depth-averaged velocity vectors (current direction and strength) and seal sightings corrected for distance and
 348 bearing during transects of the spring (20 October 2016) (a) and neap (28 October 2016) (b) tidal survey, respectively.



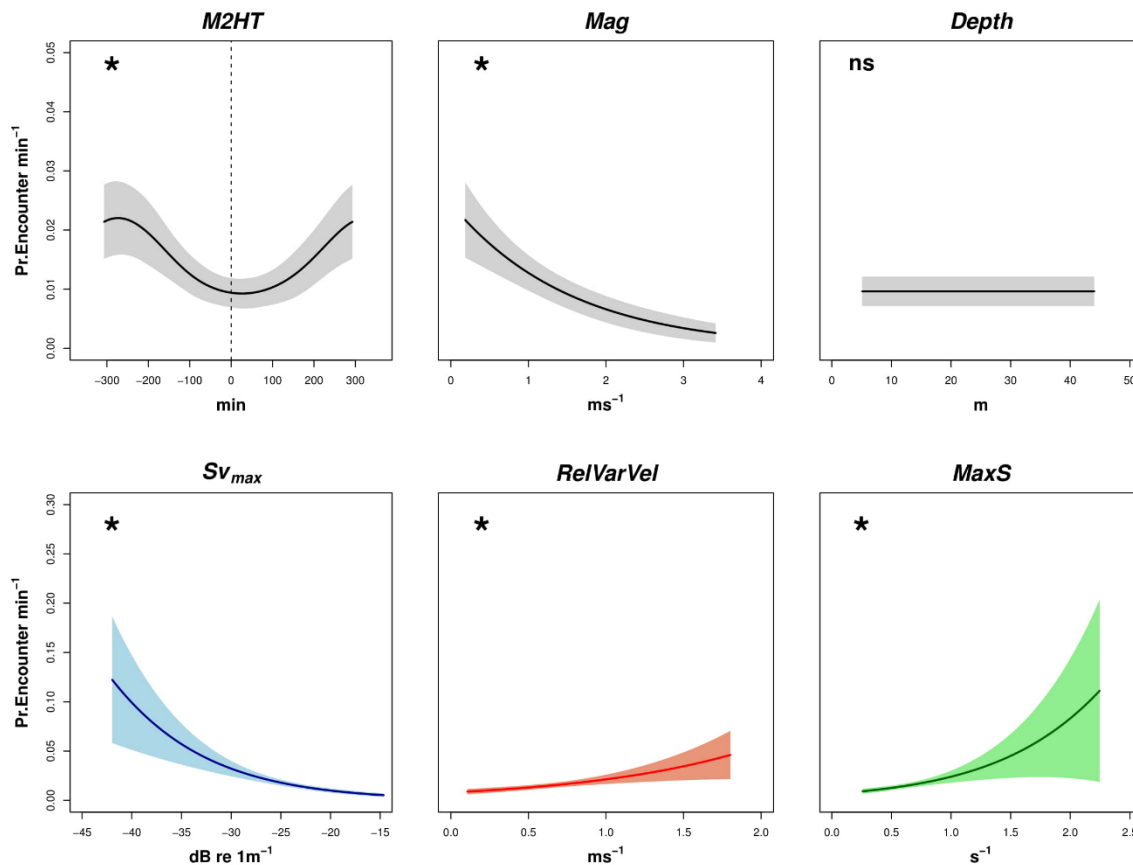
349

350 **Figure 6:** Plots of the spatial patterns of the dynamic variables applied in GAM models derived from concurrent ADCP
 351 measurements along all transects.

352 **3.2.2 Commonly-used Explanatory Variables:**

353 Significant relationships were only seen with *M2HT* ($df = 1.46, \chi^2 = 4.95, p = 0.03$) and *Mag* ($df =$
 354 $1, \chi^2 = 7.96, p < 0.01$), although the relative influence of these factors differed. The probability of
 355 encountering seals per minute showed a relatively strong and negative relationship with *Mag*, with
 356 effect sizes indicating that encounters were 7.35 times more likely in the slowest currents (Fig. 7).
 357 Whereas across all effort transects, current magnitude values ranged from $0.19 - 3.41 \text{ms}^{-1}$, seals
 358 were encountered, on average, in magnitude fields of 1.15ms^{-1} ($SD=0.75$) (Fig. S2, Supplementary
 359 Information). This further corresponds to the majority (77%) of seal encounters associated with the
 360 edges of the channel along the 20m depth contour (Fig. S3, Supplementary Information),
 361 characterized by weaker flow velocities compared to the mid-channel (Fig. 5). During slack water,

362 seals were also observed in the mid-channel. A weaker relationship was seen with *M2HT*, with
 363 effect size values showing that encounters were 1.38 times more likely during the start of the flood
 364 tide (Fig. 7).



365
 366 **Figure 7:** Modelled relationships between the probability of detecting seals per minute and environmental variables.
 367 Relationships (standard errors are indicated by shading around lines) were estimated using generalised additive models
 368 (GAMs). Different colours indicate different models. Minutes to High Tide (*M2HT*), depth-averaged current magnitude
 369 (*Mag*) and depth were modelled together in a single multivariate model. Maximum backscatter (*Sv_{max}*), mean relative
 370 variance in velocity (*RelVarVel*) and maximum shear (*MaxS*) were modelled separately in three univariate models. The
 371 statistical significance (*) or insignificance (ns) are indicated for each model.

372 **3.2.3 Novel Explanatory Variables**

373 Whilst all explanatory variables were significant (*MaxS* df = 1, $\chi^2 = 5.13$, p = 0.24; *RelVarVel* df =
 374 1, $\chi^2 = 4.46$, p = 0.35; *Sv_{max}* df=1, $\chi^2 = 13.6$, p < 0.01), large differences in effect sizes were seen.
 375 *Sv_{max}* had the highest influence: the probability of encountering seals was 22.23 times more likely
 376 in areas characterized by weaker acoustic backscatter (more negative values) (Fig. 7),

377 corresponding to the edges of the channel (Fig. 3&6). *MaxS* had the second highest influence: the
378 probability of encountering seals was 11.04 times more likely during times of maximum vertical
379 shear (Fig. 7). Finally, *RelVarVel* had the lowest influence: the probability of encountering seals was
380 4.20 times more likely in areas characterized by eddies, prevalent along the edges of the channel
381 (Figs 6&7).

382 **4. Discussion**

383 This is the first study to explore at-sea pinniped distribution patterns with concurrently
384 collected fine-scale oceanographic measurements within a tidal channel. We (1) used vessel-
385 mounted ADCP transects to characterize spatial and temporal variations in hydrodynamics within a
386 tidal channel; (2) identified several hydrodynamic metrics (macro-turbulence '*Sv_{max}*', eddies
387 '*RelVarVel*', and shear '*MaxS*') which could have ecological relevance for mobile predators using
388 these dynamic habitats and (3) showed that one of these metrics (*Sv_{max}*) had more influence than a
389 combination of more commonly-used variables (current magnitude ('*Mag*'), time to high water
390 ('*M2HW*') and depth) to detect predator associations. In combination, these results demonstrate the
391 efficacy of our survey approach to enhance environmental management at potential MRE sites by
392 showing the influence of tide-topographic processes on marine predator occupancy patterns.

393 The methodological approach described in this study, combining boat-based marine
394 mammal surveys with concurrent fine-scale ADCP measurements, is novel within energetic sites.
395 Comparative approaches combined boat-based predator surveys with moored ADCP data (Scott et
396 al., 2013), linked sightings with spatially-averaged ADCP data (IJseldijk et al., 2015), or used land-
397 based visual surveys combined with ADCP transects (Jones et al., 2014). This is not only the first
398 study of its kind on pinnipeds, but it also investigates concurrent tidal dynamics and processes on
399 comparable spatial scales to the sightings. Our approach may be highly informative within tidal
400 energy sites with only little available baseline data but could equally be adopted for other predator
401 distribution studies. For, instance, the fine-scale characterization and visualization of water column
402 characteristics and the quantification of physical structures through metrics could provide

403 oceanographic context to telemetry studies or passive and active surveys to gain a more in-depth
404 ecological understanding of animal distributions.

405 *4.1 Hydrodynamic forcing in the main channel*

406 Tidal streams are highly dynamic environments and the longevity and predictability of
407 hydrodynamic features can vary substantially, from fine spatio-temporal scales of meters and
408 seconds (e.g. bathymetry induced kolk-boils, back-eddies) to larger scale (kilometers and hours)
409 tidally-induced water movements. Here, we describe evidence of ADCP-derived metrics potentially
410 influencing seal distribution in the Narrows. The following discussion focusses on the underlying
411 hydrodynamics and physical structures arising during peak flows and provides an indication of the
412 ecological significance of seal occupancy patterns observed.

413 During periods of peak flow, seal sightings in the Narrows were concentrated along the
414 periphery of the highest flows, thereby avoiding the mid-channel and showing a preference for the
415 edges of the tidal stream (Figs. 4,5 and 7). The main flow in the mid-channel showed the highest
416 current speeds (depth-averaged current magnitude exceeded 4.5 ms^{-1} , see Figs. S4a and S4b,
417 Supplementary Information) and was dominated by macro-turbulence as evidenced by the increased
418 acoustic backscatter in this region during peak flow (Fig. 3b, and Fig. S5, Supplementary
419 Information). These regions of high backscatter are most likely clouds of micro-bubbles entrained at
420 the surface by coherent turbulent structures or “boils” and distributed throughout the water column
421 by strong turbulent mixing (Nimmo-Smith et al., 1999).

422 Marine predators performing pursuit diving of their prey are likely to forage in environments
423 where controlled diving can be maintained while maximizing foraging efficiency, limiting extensive
424 usage of the fastest-flowing currents within a tidal stream (Ladd et al., 2005; Waggitt et al., 2016a).
425 Pinnipeds mostly forage by pursuing benthic or pelagic fish with an average maximum bottom swim
426 speed for harbour seals of $2.16 (\pm 0.62) \text{ ms}^{-1}$ (Lesage et al. 1999). Flows in the mid-channel exceeded
427 these swimming speeds by a factor of two, imposing a metabolic cost associated with maintaining or

428 re-gaining control following burst dives in faster flows (unless travelling passively or “bottling” with
429 the current). In addition to the high current speeds, acoustic backscatter in the mid-channel,
430 including macro-turbulence extending down from the surface and sediment re-suspension near the
431 bed, could impair visual and auditory predatory cues. Therefore, foraging excursions into areas of
432 strong mixing are likely to be temporally limited, restricting sightings in the mid-channel in this
433 study. However, when comparing our observations with previous harbour seal telemetry studies in
434 the Narrows, patterns are in accordance. It was found that seals preferentially transited the mid-
435 channel during periods of slack tide (Sparling et al., 2017), and the spatial concentration of dive
436 density in the mid-channel was limited to periods when flow speeds were less than 1 ms^{-1} (Wood et
437 al. 2016). Finally, the presence of seals in the mid-channel during slack water indicates that depth is
438 not a driver of seal distribution patterns within the Narrows (Fig. 7).

439 *4.2 Fine-scale physical features at the edges of the channel*

440 Pinniped at-sea distribution was largely associated with the edges of the tidal channel (Fig.
441 5). The probability of encountering seals was estimated to be 22.23 times more likely in these areas
442 characterized by weaker levels of macro-turbulence (Fig. 7). The edges were further associated with
443 eddies, minimum current speeds and a higher variation in vertical shear (Figs 4 & 6). All these
444 dynamic metrics increased the probability of seal encounters (Fig. 7), justifying further discussion on
445 the hydrodynamic forcing potentially underlying edge-associations.

446 Seal occupancy patterns during periods of fast flows observed in this study show a high
447 degree of similarity to seal telemetry findings from the Narrows as noted above. During peak flows
448 (current speeds $>2\text{ms}^{-1}$), it was shown that seal dive density was concentrated at the edges of the
449 channel, on the periphery of the highest flows (Wood et al., 2016). The apparent use of low-energy
450 environments neighboring fast flows is in accordance with marine mammal use of tidal streams
451 elsewhere. At the Scottish West Coast, harbour porpoises *Phocoena phocoena* have been found to
452 spend most of their time in relatively low-energy environments adjacent to the narrow, turbulent

453 strait of the Gulf of Corryvreckan (Benjamins et al., 2016). Lower current speeds and local flow
454 reversals corresponding to the presence of eddies in the shallow areas of the Narrows may also
455 increase foraging success. For instance, in the Bay of Fundy tidal stream, Canada, cetaceans
456 *Balaenoptera physalus* and *B. acutorostrata* exhibited a consistent preference for eddy fields
457 suggesting preferred foraging along predictably occurring island wake features to exploit prey
458 aggregations retained among these eddies (Johnston et al., 2005; Johnston & Read 2007).

459 Seals in this study showed a preference for areas of maximum vertical shear, where there is
460 the largest difference between the fast-moving surface and slower near-bed flows, such as near the
461 edges of the tidal stream (Fig. 7). The increased vertical shear associated with the shallow edges of
462 the mid-channel may result in a combination of both prey being less likely to cross these areas (Čada
463 et al. 2006), and seals being able to make use of aggregated prey in these areas while maintaining
464 controlled diving (Johnston et al. 2005).

465 In addition, increased seabed roughness along the edges of the Narrows' mid-channel,
466 associated with bedrock reef and extended kelp beds, may have also influenced seal presence along
467 the 20m depth contour (Fig. 1). Rocky reefs or the presence of macro-algae and resulting habitat
468 complexity are often correlated with higher prey densities (Levin 1991), suitable for benthic
469 foraging.

470 *4.3 ADCP-derived acoustic backscatter and future directions*

471 ADCPs can determine the intensity of received echoes (total acoustic backscattering or echo
472 intensity) over a finite volume which can be converted to mean-volume backscattering strength (S_v
473 in dB; a logarithmic measure of scattering intensity) (Brierley et al. 1998). Such ADCP-derived
474 quantifications of echo intensity can give information on mid-water, bio-physical targets such as the
475 presence of dense scattering layers, including zooplankton and/or fish (Brierley et al. 1998; Deines
476 1999; Demer et al. 2000; Zedel & Cyr-Racine 2009). Applying Deines' (1999) equation, backscatter
477 calculations accounted for time-varying gain, absorption loss, transmit pulse length and beam-

478 specific sensitivity coefficients, making it a more robust measure compared to raw echo intensity
479 which can be more easily extracted from ADCP data. In this study, backscatter (Sv_{max}) was used as an
480 indicator for surface bubble entrainment resulting from macro-turbulence as well as sediment
481 resuspension near the bed. The scattering could not be identified as being of biological origin in the
482 absence of acoustic multi-frequency techniques, although the backscatter patterns were more
483 characteristic of entrained bubbles. Understanding foraging opportunities for top predators in such
484 dynamic environments requires the assessment of real-time prey landscapes and the reliable
485 isolation of biological targets in highly turbulent environments (Lavery et al. 2009; Fraser et al.,
486 2017).

487 Additionally, prey behavior may be similarly influenced by hydrodynamic forcing. High
488 current speeds largely exceeding most fish cruising swim speeds (generally not exceeding 2 ms^{-1} ;
489 Videler & Wardle 1991) in the mid-channel during peak flows may equally impose a metabolic cost
490 to prey unless they actively seek the channel as a means of transport. Further, strong vertical
491 turbulent conditions and high flows in the mid-channel could provide a mechanism to disorient prey
492 and may impact on school cohesion (Zamon 2001; Liao 2007; Robinson et al. 2007). This would
493 increase vulnerability to predators as harbour seal foraging success on schooling fish has been
494 shown to be increased following school break-up, when a small group or a single prey item is
495 separated, thus avoiding the confusion effect of the school (Kilian et al. 2015). Finally, patches of
496 high vertical shear were found near the bed in the central part of the channel and fish may also
497 avoid this part of the tidal stream during strong flows to avoid vertical displacement as sudden
498 changes in pressure may lead to barotrauma-related injuries (Brown et al. 2009).

499 Future studies in the Narrows would highly benefit from the collection of multi-frequency
500 acoustic backscatter data (e.g. EK 80/AZFP echosounder data) to help distinguish physical from
501 biological sources of scattering (using dB difference techniques) and to capture spatio-temporal
502 patterns in prey variability. The combination of hydroacoustic tools (ADCPs and calibrated
503 echosounders) could help explore the mechanisms underlying prey behavior in the Lough following

504 the extraction of fish and water velocities (Zedel & Cyr-Racine 2009) to eventually understand the
505 entire suite of bio-physical drivers underlying seal habitat use in the Narrows.

506 *4.4 Conclusion and implications*

507 The novelty of our approach lies in the determination of fine-scale physical metrics
508 influencing predator occupancy patterns previously not considered in these extremely energetic
509 habitats. The use of ADCPs in combination with other survey methodologies is still inadequately
510 represented given its potential value in understanding a species' behavioral ecology. Our approach
511 can be adapted to other tidal energy sites, specifically where baseline data is limited, to inform the
512 environmental impact process from the start. It appears to be one of the most practical and cost-
513 effective approaches to streamline the EIA process in the early stages of the consenting process.
514 Baseline studies of this kind are necessary to detect trends and to determine the spatial scales at
515 which to further investigate more detailed predator behavior within these energetic environments.

516 Developers tasked with undertaking a series of marine mammal sighting surveys as part of
517 EIAs at MRE sites may adopt this methodological approach. Repeat-transect surveys of this kind
518 allow to simultaneously inform hydrodynamic and marine mammal site characterization, therefore
519 maximizing resources (data quality vs survey costs) allocated to EIAs. An increased number of
520 transects (ideally during different times of the year) could improve the resolution often required for
521 EIAs, such as applying the detection function to obtain animal density and abundance estimates,
522 whilst also providing more detailed information on seasonal variability in flows and predator
523 associations.

524 Our results showed that on average, seals were encountered in current magnitude fields of
525 1.15 ms^{-1} ($SD=0.75$) and avoided areas of extreme acoustic backscatter, such as the mid-channel
526 during peak flows. This may have implications for tidal energy site selection as turbines are generally
527 placed within more predictable environments characterized by fast ($>2 \text{ ms}^{-1}$), uni-directional flows
528 and lower degrees of terrain ruggedness (to reduce bathymetry-induced turbulence and issues with

529 foundation deployment). Seals sighted in the mid-channel, areas where such characteristics would
530 be fulfilled, were highest during slack water when tidal turbines are less likely to be operating at full
531 capacity (or at all) and therefore risk from interactions (e.g. collision) is deemed to be low.

532

533 **Authors contributions**

534 LL and LK conceived the ideas and designed the study; LK coordinated data acquisition and managed
535 the project. LL collected the data and LL, WAMNS and JJW performed the analysis and interpreted
536 the results. LL drafted the manuscript. All authors contributed critically to the drafts and gave final
537 approval for publication.

538 **Acknowledgements**

539 This study is part of the PowerKite project which has received funding from the European Union's
540 Horizon 2020 research and innovation programme under grant agreement No 654438. James
541 Waggitt is supported through the Marine Ecosystems Research Programme (MERP: NE/L003201/1)
542 which is funded by the Natural Environment Research Council and the Department for Environment,
543 Food & Rural Affairs (NERC/DEFRA). We would particularly like to acknowledge the support given by
544 Pál Schmitt during data collection. We also wish to thank Jeremy Rogers, Simon Rogers and Oliver
545 Rogers from Cuan Marine Services for boat time, seamanship and their in-depth knowledge of the
546 Narrows necessary for this study's survey methodology. Finally, we'd like to thank Laura Hobbs and
547 Andrew S. Brierley for advice on backscatter calculations. The authors declare no conflict of interest.

548 **Data accessibility**

549 The data used in this manuscript will be deposited in the Dryad Digital Repository.

550 **References**

- 551 Benjamins, S., Dale, A.C., Hastie, G., Waggitt, J.J., Lea, M.-A., Scott, B. & Wilson, B. (2015a) Confusion Reigns? A
552 Review of Marine Megafauna Interactions with Tidal-Stream Environments. *Oceanography and Marine
553 Biology: An Annual Review*, **53**, 1–54.
- 554 Benjamins, S., Macleod, A., Greenhill, L. & Wilson, W. (2015b) Surveying marine mammals in nearby tidal

555 energy development sites: a comparison. *Proceedings of the 11th European Wave and Tidal Energy*
556 *Conference 6-11th Sept 2015, Nantes, France*

557 Benjamins, S., Dale, A., Van Geel, N. & Wilson, B. (2016) Riding the tide: Use of a moving tidal-stream habitat
558 by harbour porpoises. *Marine Ecology Progress Series*, **549**, 275–288.

559 Benjamins, S., van Geel, N., Hastie, G., Elliott, J. & Wilson, B. (2017) Harbour porpoise distribution can vary at
560 small spatiotemporal scales in energetic habitats. *Deep Sea Research Part II: Topical Studies in*
561 *Oceanography*, **141**, 191–202.

562 Buckland, S.T., Anderson, D.R., Burnham, K.P., Laake, J.L., Borchers, D.L. & Thomas, L. (2001) *Introduction to*
563 *Distance Sampling: Estimating Abundance of Biological Populations*.

564 Brierley, A.S., Brandon, M.A. & Watkins, J.L. (1998) An assessment of the utility of an acoustic Doppler current
565 profiler for biomass estimation. *Deep Sea Research Part I: Oceanographic Research Papers*, **45**, 1555–73.

566 Brown, R.S., Carlson, T.J., Welch, A.E., Stephenson, J.R., Abernethy, C.S., Ebberts, B.D., Langeslay, M.J.,
567 Ahmnan, M.L., Feil, D.H., Skalski, J.R. & Townsend, R.L. (2009). Assessment of barotrauma from rapid
568 decompression of depth- acclimated juvenile Chinook salmon bearing radiotelemetry transmitters.
569 *Transactions of the American Fisheries Society* **138**, 1285–1301.

570 Čada, G., Loar, J., Garrison, L., Fisher, R., Jr & Neitzel, D. (2006). Efforts to reduce mortality to hydroelectric
571 turbine- passed fish: locating and quantifying damaging shear stresses. *Environmental Management* **37**,
572 898–906.

573 Deines, K.L. (1999) Backscatter estimation using Broadband acoustic Doppler current profilers. *Proceedings of*
574 *the IEEE Sixth Working Conference on Current Measurement (Cat. No.99CH36331)*, 1–5.

575 Demer, D.A., Barange, M. & Boyd, A.J. (2000) Measurements of three-dimensional fish school velocities with
576 an acoustic Doppler current profiler. *Fisheries Research*, **47**, 201–214.

577 Embling, C.B., Illian, J., Armstrong, E., van der Kooij, J., Sharples, J., Camphuysen, K.C.J. & Scott, B.E. (2012)
578 Investigating fine-scale spatio-temporal predator-prey patterns in dynamic marine ecosystems: a
579 functional data analysis approach. *Journal of Applied Ecology*, **49**, 481–492.

580 Epler, J., Polagye, B. & Thomson, J. (2010) Shipboard acoustic Doppler current profiler surveys to assess tidal
581 current resources. *OCEANS 2010, MTS/IEEE Seattle, USA*.

582 Evans, P., Armstrong, S., Wilson, C., Fairley, I., Wooldridge, C. & Masters, I. (2013) Characterisation of a Highly
583 Energetic Tidal Energy Site with Specific Reference to Hydrodynamics and Bathymetry. *In Proceedings of*
584 *the 10th European wave and tidal energy conference (EWTEC 2013)*.

585 Fong, D.A. & Monismith, S.G. (2004) Evaluation of the accuracy of a ship-mounted, bottom-tracking ADCP in a
586 near-shore coastal flow. *Journal of Atmospheric and Oceanic Technology*, **21**, 1121–1128.

587 Fox, C.J., Benjamins, S., Masden, E. & Miller, R. (2017) Challenges and opportunities in monitoring the impacts
588 of tidal-stream energy devices on marine vertebrates. *Renewable and Sustainable Energy Reviews*, **81**,
589 Part 2, 1926-1938

590 Fraenkel, P. (2004) Marine Current Turbines: an emerging technology. *Paper for Scottish Hydraulics Study*
591 *Group Seminar in Glasgow on 19 March 2004 Renewable Energy – Hydraulic Applications – Theory and*
592 *Practice*, 1–10.

593 Fraser, S., Nikora, V., Williamson, B.J. & Scott, B.E. (2017) Automatic active acoustic target detection in
594 turbulent aquatic environments. *Limnol. Oceanogr. Methods*, **15**, 184–199.

595 Goddijn-Murphy, L., Woolf, D.K. & Easton, M.C. (2013) Current patterns in the inner sound (Pentland Firth)
596 from underway ADCP data. *Journal of Atmospheric and Oceanic Technology*, **30**, 96–111.

597 Harwood, J., Stokes, K. (2003) Coping with uncertainty in ecological advice: lessons from fisheries. *Trends Ecol*
598 *Evol* **18**, 617–22.

599 Hastie, G.D., Russell, D.J.F., Benjamins, S., Moss, S., Wilson, B. & Thompson, D. (2016) Dynamic habitat
600 corridors for marine predators; intensive use of a coastal channel by harbour seals is modulated by tidal
601 currents. *Behavioral Ecology and Sociobiology*, **70**, 2161–2174.

602 IJsseldijk, L. L., Camphuysen, K. C. J., Nauw, J. J., & Aarts, G. (2015). Going with the flow: Tidal influence on the
603 occurrence of the harbour porpoise (*Phocoena phocoena*) in the Marsdiep area, The Netherlands.
604 *Journal of Sea Research*, **103**, 129–137.

605 Jeffcoate, P., Whittaker, T., Boake, C. & Elsäßer, B. (2016) Field tests of multiple 1/10 scale tidal turbines in
606 steady flows. *Renewable Energy*, **87**, 240–252.

607 Johnston, D.W. & Read, A.J. (2007) Flow-field observations of a tidally driven island wake used by marine
608 mammals in the Bay of Fundy, Canada. *Fisheries Oceanography*, **16**, 422–435.

609 Johnston, D.W., Thorne, L.H. & Read, A.J. (2005) Fin whales *Balaenoptera physalus* and minke whales
610 *Balaenoptera acutorostrata* exploit a tidally driven island wake ecosystem in the Bay of Fundy. *Marine*
611 *Ecology Progress Series*, **305**, 287–295.

612 Jones, A.R., Hosegood, P., Wynn, R.B., De Boer, M.N., Butler-Cowdry, S. & Embling, C.B. (2014) Fine-scale
613 hydrodynamics influence the spatio-temporal distribution of harbour porpoises at a coastal hotspot.
614 *Progress in Oceanography*, **128**, 30–48.

615 Kilian, M., Dehnhardt, G., Hanke, F.D. (2015) How harbour seals (*Phoca vitulina*) pursue schooling herring.
616 *Mammal Biol* **80**, 385–389

617 Kregting, L. & Elsäßer, B. (2014) A Hydrodynamic Modelling Framework for Strangford Lough Part 1: Tidal
618 Model. *Journal of Marine Science and Engineering*, **2**, 46–65.

619 Kregting, L., Elsäßer, B., Kennedy, R., Smyth, D., O'Carroll, J. & Savidge, G. (2016) Do changes in current flow as
620 a result of arrays of tidal turbines have an effect on benthic communities? *PLoS ONE*, **11**, 1–14.

621 Ladd, C., Jahncke, J., Hunt, G.L., Coyle, K.O. & Stabeno, P.J. (2005) Hydrographic features and seabird foraging
622 in Aleutian Passes. *Fisheries Oceanography*, **14**, 178–195.

623 Lavery, A. C., Chu, D. & Moum, J.N. (2009) Measurements of acoustic scattering from zooplankton and oceanic
624 microstructure using a broadband echosounder. *ICES Journal of Marine Science*, **67**, 379–394.

625 Lesage, V., Hammil, M.O., Kovacs, K.M., (1999). Functional classification of harbor seal (*Phoca vitulina*) dives
626 using depth profiles, swimming velocity, and an index of foraging success. *Can. J. Zool.* **77**, 74–87.

627 Levin, P.S. (1991) Effects of microhabitat on recruitment variation in a Gulf of Maine reef fish. *Marine Ecology*
628 *Progress Series*, **75**, 183–189.

629 Liao, J.C. (2007) A review of fish swimming mechanics and behaviour in altered flows. *Philosophical*

630 *transactions of the Royal Society of London. Series B, Biological sciences*, **362**, 1973–1993.

631 Lu, Y. & Lueck, R.G. (1999) Using a broadband ADCP in a tidal channel. Part I: Mean flow and shear. *Journal of*
632 *Atmospheric and Oceanic Technology*, **16**, 1556–1567.

633 Nimmo-Smith, W.A.M., Thorpe, S.A. & Graham, A. (1999) Surface effects of bottom-generated turbulence in a
634 shallow tidal sea. *Nature*, **400**, 251–254.

635 Polagye, B. & Thomson, J. (2013) Tidal energy resource characterization: methodology and field study in
636 Admiralty Inlet, Puget Sound, US. *Proceedings of the Institution of Mechanical Engineers, Part A: Journal*
637 *of Power and Energy*, **227**, 352–367.

638 R Core Team (2014) R: A Language and Environment for Statistical Computing. R Foundation for Statistical
639 Computing, Vienna, Austria.

640 Robinson, C.J., Gómez-Aguirre, S. & Gómez-Gutiérrez, J. (2007). Pacific sardine behaviour related to tidal
641 current dynamics in Bahía Magdalena, México. *Journal of Fish Biology*, **71**, 200–218.

642 Savidge, G., Ainsworth, D., Bearhop, S., Christen, N., Elsässer, B., Fortune, F.,... & Whittaker, T.J.T. (2014)
643 Strangford Lough and the SeaGen Tidal Turbine. *M. A. Shields, A. I. L. Payne (eds), Marine Renewable*
644 *Energy Technology and Environmental Interactions, Humanity and the Sea*

645 Scott, B. E., Webb, A., Palmer, M. R., Embling, C. B., & Sharples, J. (2013). Fine scale bio-physical oceanographic
646 characteristics predict the foraging occurrence of contrasting seabird species; Gannet (*Morus bassanus*)
647 and storm petrel (*Hydrobates pelagicus*). *Progress in Oceanography*, **117**, 118–129.

648 Shields MA, Woolf DK, Grist EP, Kerr SA and others (2011) Marine renewable energy: the ecological
649 implications of altering the hydrodynamics of the marine environment. *Ocean Coast Manag*, **54**, 2–9

650 Simpson, J.H., Mitchelson-Jacob, E.G. & Hill, A.E. (1990) Flow structure in a channel from an acoustic Doppler
651 current profiler. *Continental Shelf Research*, **10**, 589–603.

652 Sparling, C., Lonergan, M., & McConnell, B. (2017). Harbour seals (*Phoca vitulina*) around an operational tidal
653 turbine in Strangford Narrows: No barrier effect but small changes in transit behaviour. *Aquatic*
654 *Conservation: Marine and Freshwater Ecosystems*, 1–11.

655 Thomas, L., Buckland, S.T., Rexstad, E.A., Laake, J.L., Strindberg, S., Hedley, S.L., Bishop, J.R.B., Marques, T.A. &
656 Burnham, K.P. (2010) Distance software: Design and analysis of distance sampling surveys for estimating
657 population size. *Journal of Applied Ecology*, **47**, 5–14.

658 Videler, J.J. & Wardle, C.S. (1991). Fish swimming stride by stride: speed limits and endurance. *Reviews in Fish*
659 *Biology and Fisheries* **1**, 23–40.

660 Waggitt, J.J., Cazenave, P.W., Torres, R., Williamson, B.J. & Scott, B.E. (2016a) Predictable hydrodynamic
661 conditions explain temporal variations in the density of benthic foraging seabirds in a tidal stream
662 environment. *ICES Journal of Marine Science*, **73**, 2677–2686.

663 Waggitt, J.J., Cazenave P.W., Torres, R., Williamson, B. & Scott, B. (2016b) Quantifying pursuit-diving seabirds
664 use of fine-scale physical features in tidal stream environments. *Journal of Applied Ecology*, **53**, 1653–
665 1666.

666 Waggitt, J.J., Dunn, H.K., Evans, P.G.H., Hiddink, J.G., Holmes, L.J., Keen, E., Murcott, B.D., Piano, M., Robins,
667 P.E., Scott, B.E., Whitmore, J., Veneruso, G. (2017a) Regional-scale patterns in harbour porpoise
668 occupancy of tidal stream environments. *ICES Journal of Marine Science*, doi:10.1093/icesjms/fsx164

669 Waggitt, J.J., Robbins, A.M.C., Wade, H.M., Masden, E.A., Furness, R.W., Jackson, A.C. & Scott, B.E. (2017b)
670 Comparative studies reveal variability in the use of tidal stream environments by seabirds. *Marine Policy*,
671 **81**, 143–152.

672 Waggitt, J.J. & Scott, B.E. (2014) Using a spatial overlap approach to estimate the risk of collisions between
673 deep diving seabirds and tidal stream turbines: A review of potential methods and approaches. *Marine*
674 *Policy*, **44**, 90–97.

675 Wilson, B., Batty, R.S., Daunt, F. & Carter, C. (2007) Collision risks between marine renewable energy devices
676 and mammals, fish and diving birds. *Report to the Scottish Executive.Scottish Association for Marine*
677 *Science, Oban, Scotland, PA37 1QA.*, 1–105.

678 Wood, J., Joy, R. & Sparling, C. (2016) Harbor Seal – Tidal Turbine Collision Risk Models. An Assessment of
679 Sensitivities. *Prepared for PNNL / DOE by SMRU Consulting.*

680 Woods, S. (2006) Generalized Additive Models: An Introduction with R. *CRC Texts in Statistical Science.*

- 681 Woods, S. (2017) Mixed GAM Computation Vehicle with GCV/AIC/REML Smoothness Estimation.
- 682 Zamon, J.E. (2001) Seal predation on salmon and forage fish schools as a function of tidal currents in the San
683 Juan Islands, Washington, USA. *Fisheries Oceanography*, **10**, 353–366.
- 684 Zedel, L. & Cyr-Racine, F.-Y. (2009) Extracting fish and water velocity from Doppler profiler data. *ICES Journal of*
685 *Marine Science*, **66**, 1846–1852.
- 686